Pergamon

0273-1177(94)00108-1

Adv. Space Res. Vol. 15, No. 8/9, pp. (8/9)285–(8/9)296, 1995

0273–1177/95 $9.50 + 0

ULTRA LOW FREQUENCY WAVES AT THE EARTH'S BOW SHOCK

C. T. Russell and M. H. Farris

Institute of Geophysics and Planetary Physics, University of California, Los Angeles, CA 90024-1567, U.S.A.

ABSTRACT

The Earth's bow shock is a bountiful generator of waves. Some of these waves have group velocities that exceed the solar wind velocity directed into the shock and can propagate upstream against the flow. Upstream whistlers observed close to one Hertz in the spacecraft frame have been seen many Earth radii upstream. A second whistler mode wave, called the precursor, propagates upstream along the shock normal but is phase standing in the solar wind flow. The damping of both whistler mode waves is consistent with Laudau damping. At low Mach numbers the precursor is connected to the non-coplanarity component in the shock ramp. At higher Mach numbers the upstream waves cannot propagate upstream and ion reflection becomes more important in providing free energy for wave particle interactions. The non-coplanarity component is still present but it now initiates a downstream wave train. Generally the waves just downstream from the bow shock are left hand circularly polarized ion cyclotron waves propagating along the magnetic field at the Alfven velocity. When the upstream Mach number is high and the helium content of the plasma is high, mirror mode waves are observed.

INTRODUCTION

One aspect of the physics of collisionless shocks is well understood. The Rankine-Hugoniot equations [1,2] allow one to accurately predict the average downstream state from the average upstream state if one knows the strength of the shock and if a polytropic equation of state can be used. This has been tested for typical plasma conditions for the Earth's bow shock [3]; for the Venus bow shock [4]; for interplanetary shocks [5] and for very high beta shocks [6]. Figure 1 illustrates the behavior of the density ratio across the shock as a function of the magnetosonic Mach number for a beta of unity and an angle between the shock normal and the upstream magnetic field, θ_{BN}, of 90°. Unless beta is low this behavior does not depend greatly on θ_{BN}. We see that the density ratio increases with increasing Mach number to an asymptotic value of 4 which is appropriate for a polytropic index of 5/3. Once the shock reaches moderate Mach numbers little further compression of the plasma occurs.

The magnetic field similarly reaches an asymptotic value but this value is sensitive to the direction of the upstream magnetic field as shown in Figure 2. The temperature behaves quite differently as shown in Figure 3. It increases monotonically with Mach number and does not reach an asymptotic limit. Thus

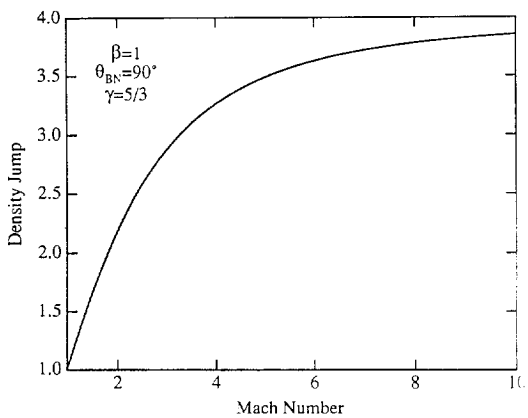

Fig. 1 Jump in plasma density as a function of the upstream magnetospheric Mach number for beta equal to unity $\theta_{BN} = 90°$ and $\gamma = 5/3$.

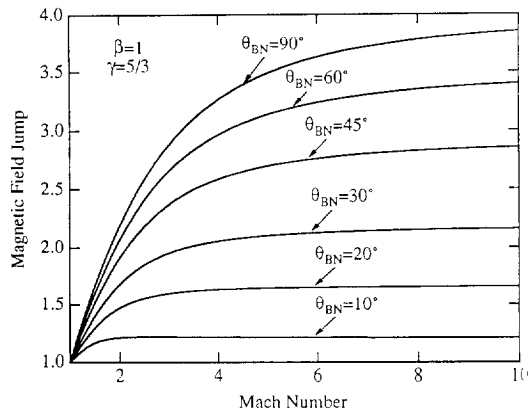

Fig. 2 Jump in magnetic field strength as a function of Mach number for the same condition as Fig. 1.

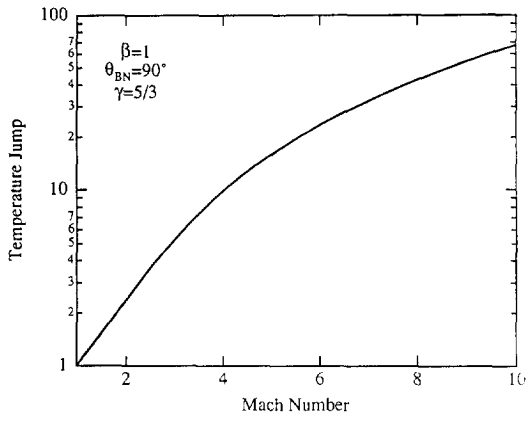

Fig. 3 Jump in temperature as a function of Mach number for the same conditions as Fig. 1.

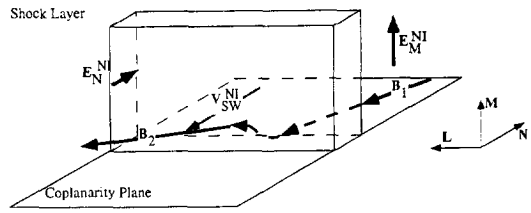

Fig. 4 Schematic of the crossing of the shock by the magnetic field in the presence of a non-coplanarity component of the magnetic field. In this frame, the normal incidence frame, the solar wind velocity is along the shock normal. Electrons, that follow the magnetic field line are carried in the direction of the interplanetary electric field by the jog and hence do not feel the full potential drop across the shock. Ion which proceed straight through the shock see the full decelerating (for them) electric potential.

even though the plasma is compressed to near its limiting value, greater and greater dissipation occurs with increasing Mach number. Since shock heating covers such a wide range we might not expect a single mechanism to be able to provide the requisite dissipation at all Mach numbers. The Rankine-Hugoniot equations provide no help in this regard because they do not tell how the requisite dissipation is provided, nor even the partitioning of the thermal energy among the plasma constituents. In order to determine the relative heating and the mechanisms that provide it, we must understand the microprocess of the shock. Some of these microprocesses involve waves, the subject of this review, and some do not. An important mechanism in this regard is the transport of electrons across the shock via the noncoplanar component of the magnetic field. Since the acceleration of electrons is most strongly affected by this process we will review it here.

The existence and importance of the non-coplanar component of the magnetic field at the shock has been treated by many authors [7-11]. Figure 4 shows the components of the vector magnetic field in shock normal components for a subcritical, quasi-perpendicular shock. The M component is in the plane of the shock and perpendicular to the projection of the upstream field on the shock. In the shock ramp, as if to terminate the upstream precursor, there is a negative deviation of BM. This is the non-coplanarity component. Its sense in this coordinate system for a fast shock is such that the product of the average normal component and the noncoplanar component is negative. (For a slow shock this product should be positive.)

The importance of the noncoplanar component of the magnetic field can be illustrated with the aid of Figure 5 which illustrates the path taken by the upstream magnetic field through the shock. Electrons are tied to these field lines because their gyro radii are small compared to thickness of the shock. As the electrons move through the shock they make a jog which move them in the direction of the interplanetary electric field, E_M^{NI}, and they lose energy, but as they penetrate the shock they also are accelerated by the electric potential barrier that shows the ions. As a result they are accelerated by some (about 10%) but not all of the E_N^{NI}. The ions which pass straight through the shock see the full effect of E_N^{NI}.

Another important microprocess at the shock that does not involve waves per se is ion reflection. The ion reflection process can be explained with the help of Figure 6. If the shock potential is small then the ions whose distribution is sketched in the top panel can all easily pass through the potential barrier. In the process they are slowed and heated but they all pass through as illustrated in the next lower panel. When the shock potential is a large fraction of the incoming ion energy, not all the ions can pass through the potential barrier. Some (the slower ones) are reflected back into the solar wind only to gyrate around the magnetic field and drift with the upstream electric field back into the sheath (second panel from the bottom). Finally, wave particle interactions isotropize the distribution. Thus although the dissipation

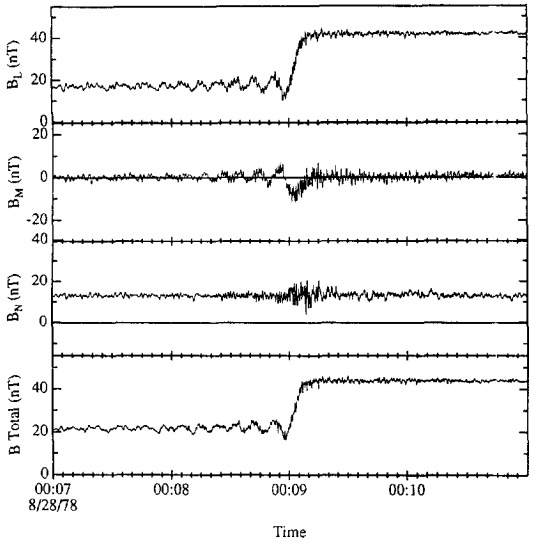

Fig. 5 Magnetic field measurements across a subcritical quasi perpendicular shock displayed in boundary normal coordinates on 8/28/78. Upstream conditions were $M_{ms}=1.53$, $\beta=0.07$ and $\theta_{BN} = 58°$.

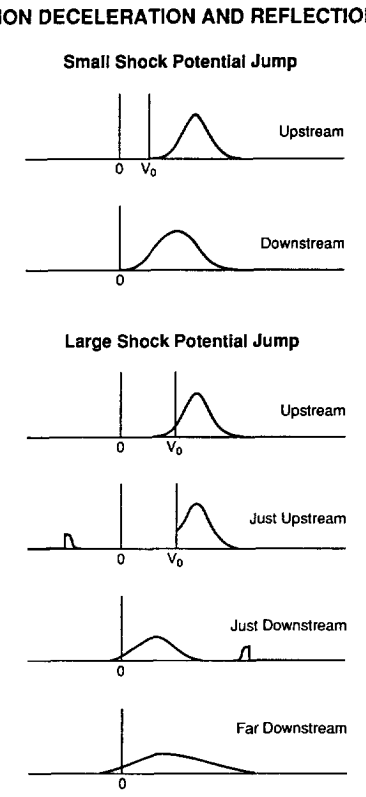

Fig. 6 Schematic in phase space of the effect of the electric potential on the ion distribution function along the N direction for subcritical (top) and supercritical (bottom) conditions. V_o is the critical velocity that allows an ion to just pass through the electrical potential barrier.

process does not involve waves, it certainly leads to particle distributions that are unstable to wave growth as we shall discuss in the following sections of this review.

One final topic that we wish to discuss is the switch-on shock which occurs, in sensu stricto, only for θ_{BN} equal to zero, but in practice can be defined for a range of θ_{BN}. At low Mach numbers and betas, a tangential magnetic field can appear even though there was no tangential magnetic field upstream. For non-zero θ_{BN} the manifestation of a switch-on shock is a large increase in the tangential component. We have found one such case of a switch-on shock in the ISEE data. (Farris et al. 1994). It is notable not only for the switch on of the tangential magnetic field but it will also be important in discussing the phase standing precursor.

In this review we examine the generation of ultra low frequency waves at the Earth's bow shock. Ultra low frequencies by definition have periods longer than 0.3s. In the plasma frame we will find that these waves occur at frequencies well less than the electron gyro frequency and most often less than the ion gyro frequency.

PROPAGATING UPSTREAM WHISTLERS

Whistler mode waves with frequencies of about 1 Hz were found well upstream of the Earth's bow shock in 1971 [13]. Later, based on observations of these same waves closer to the bow shock, they were identified as generated at the bow shock with group velocities that allowed them to propagate upstream against the solar wind flow [14]. These waves were found to be right handed when the component of the solar wind velocity along the wave normal was less than the phase velocity of the wave and to be left

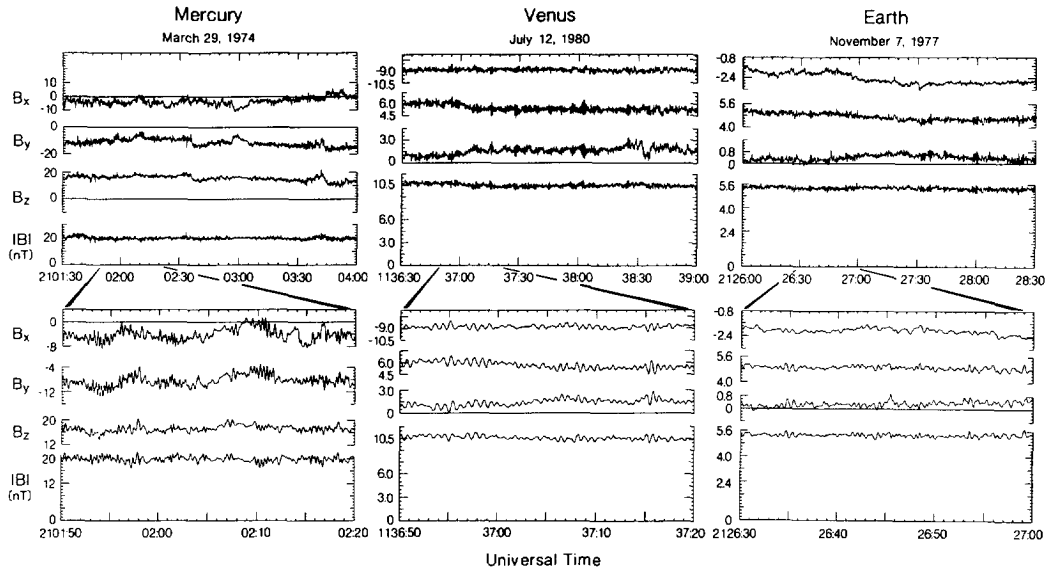

Fig. 7 Upstream whistlers at Mercury, Venus, and Earth.

handed when the component of the solar wind velocity was greater than the phase velocity but less than the group velocity. Example of these waves seen at Mercury, Venus and the Earth are seen in Figure 7 [15]. Some controversy arose over the source of these waves when early ISEE observations were obtained [16] and a new interpretation was developed based on the instability of electron beams in the foreshock [17]. More recent studies support the original interpretation of shock generation. Most importantly, the waves are largest near the shock [18].

Recent modeling the growth rates of these waves in the upstream electron beams [19] does not support the earlier assertion of wave growth [17]. All waves studied damped as they propagated into the solar wind. These waves have also been found in the Saturn foreshock but at a much lower frequency [20].

The properties of the waves are fairly well understood. The waves are elliptically to circularly polarized depending on how closely they propagate along the magnetic field. Generally the waves are fairly well guided by the field if only because waves at large θ_{Bk} will Landau dump more quickly. The frequency of the waves in the plasma frame is much greater than the proton gyro frequency but less than the lower hybrid frequency.

While we understand well the propagation of these waves, we understand less well how these waves are generated by the shock. We do not understand what instability (probably) of the electrons generates the waves or why the waves generally propagate close to but not exactly along the magnetic field. Whatever the source it seems to be an important microprocess for the shock because the waves are moderately strong and fairly ubiquitous. They seem only to be absent when the propagation direction is so close to being tangent to the shock surface that the solar wind convects the waves across the shock and downstream of it.

PHASE STANDING WHISTLER PRECURSORS

When the Mach number of a fast mode shock is low, whistler mode waves can run out in front of it because the whistler mode velocity exceeds that of the shock. One example of this phenomenon was discussed above. A district phenomenon is the phase standing whistler precursor observed for subcritical shocks. By subcritical we mean that the downstream flow speed is greater than the downstream sound speed. Figure 8 shows the magnetic field strength observed across five low Mach number shocks, ordered by increasing Mach number as normalized by the critical Mach number. The horizontal scale is the distance along the shock normal measured in ion inertial lengths which is the same as the gyro radius of an ion moving at the Alfven velocity. Figure 8 illustrates many important features of

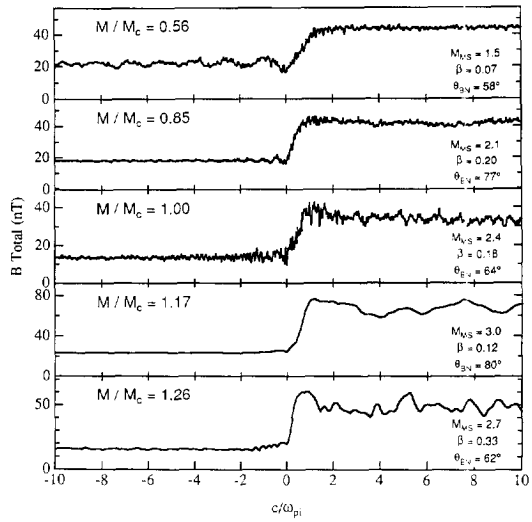

Fig. 8 Magnetic field strength as a function of distance from the shock ramp measured in ion inertial lengths for 5 shocks of increasing Mach number. The Mach number is measured relative to the critical Mach number at which the downstream flow velocity equals the sound speed.

collisionless shocks. First, as seen in the top two panels whistler precursors, are found on the upstream side of the shock ramp. These waves propagate along the normal and maintain a constant phase with respect to the shock ramp. The middle panel in contrast shows an example of propagating upstream whistlers at about 1 Hz. These propagate more nearly along the upstream magnetic field direction. At higher Mach numbers the upstream waves disappear and a foot appears at the base of the ramp. Downstream of the shock the amplitude of the ULF waves increases with increasing Mach number. For all Mach numbers shown here the thickness of the shock is roughly the same, close to an ion inertial length.

The wavelength of the phase standing precursor is well understood. Since it phase stands on the shock and propagates along the shock normal we can calculate the wavelength if we know the solar wind conditions. This calculation is performed for a number of low Mach number shocks in Figure 9 and compared with observations. The agreement is very good.

We do not understand the thickness of the shock as well. One might assume from the top 2 panels of Figure 8 that the thickness of the shock was related to the wavelength of the precursor - perhaps being

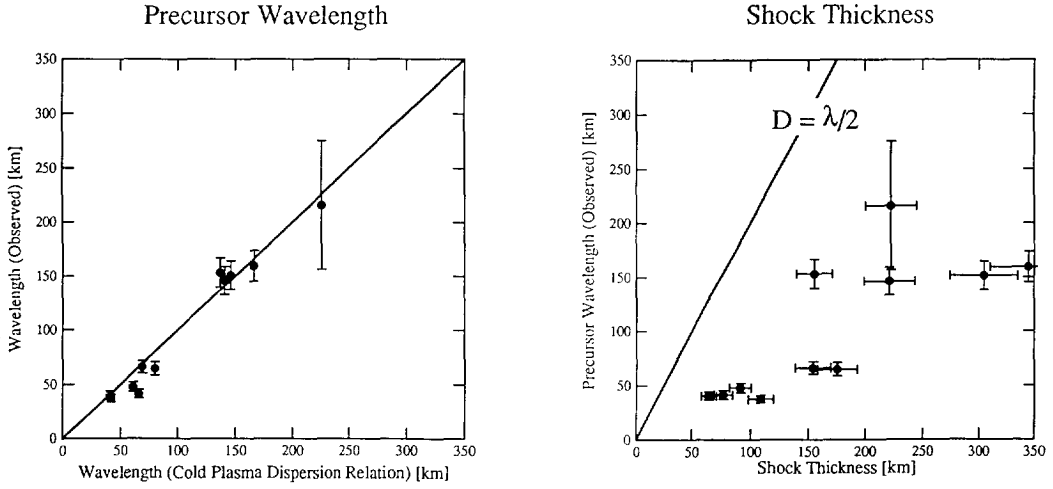

Fig. 9 The observed wavelength of the precursor plotted versus the expected wavelength on the left, and versus the shock thickness on the right. The shock thickness is measured from the minimum field strength to the maximum.

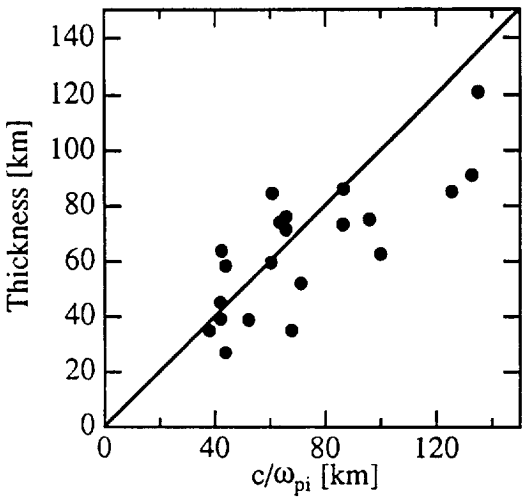

Fig. 10 The thickness of all nearly perpendicular shocks plotted versus the size of an ion inertial length for the crossing. All shocks have an angle between the IMF and the shock normal of greater than 80°.

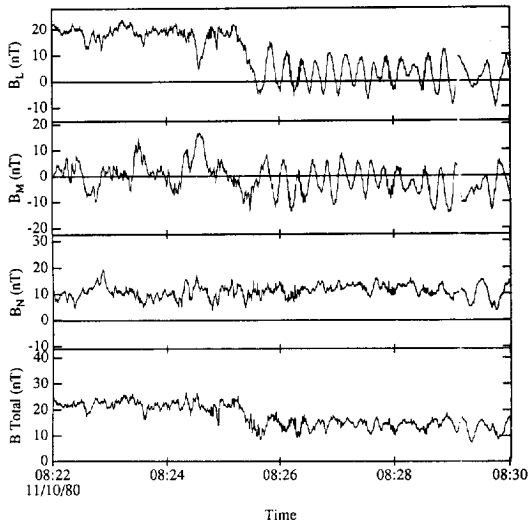

Fig. 11 Magnetic field measurements of a subcritical nearly parallel shock (a switch on shock) in shock normal coordinates. Upstream conditions were M_{ms} = 1.59, β=0.19 and θ_{BN}=17.

one-half of the wavelength. However, Figure 9 clearly shows that this hypothesis is not true. The shock is much thicker than one-half a precursor wavelength and shock and at best seems only weakly correlated with it. Thus, dissipation processes within the shock ramp appear to be most strongly responsible for determining the shock thickness.

It has also been speculated that perpendicular and nearly perpendicular shocks may be much thinner than other shocks. Even though it is difficult for us to determine very accurate shock normals when the IMF is perpendicular to the shock normal we can examine all shocks in the vicinity of this point and look for evidence of any thin shocks. This is done in Figure 10, and we can see no evidence for thin shocks. The best estimate of the thickness of these shocks is the ion inertial length.

Let us now return to the properties of the precursor having established that the precursor has little to do with the shock thickness. Figure 11 shows our longest enduring precursor for a nearly parallel shock which has been interpreted as a switch-on shock [12]. The switch-on nature of the shock can be seen in the B_L component which lies in the plane of the shock parallel to the average upstream magnetic field. Upstream on the right of the figure, this field component averages to near zero, whereas it is large and steady downstream. The steadiness of the downstream field also shows that the precursor wave is standing (or propagating upstream) and is not convected through the shock.

Most precursor waves damp more rapidly than the wave shown here. Gary and Mellott [21] have proposed that the waves damp as they propagate away from the shock through Landau damping. Figure 12 shows calculated damping length normalized to precursor wavelengths and the calculated damping rates for the precursors we have observed. The precursor of Figure 11 is the one that shows almost zero damping. These results are similar both qualitatively and quantitatively to the predicted rates.

BEAM GENERATED UPSTREAM WAVES

As the strength of the shock increases above the critical Mach number the number of ions reflected by the shock potential also increases. This mechanism provides much of the dissipation required by the Rankine-Hugoniot equations. For quasi perpendicular shocks, these ions are turned around by the upstream IMF and drift back through the shock with the EXB drift of the solar wind. These particles then contribute to the wave generation process downstream. For quasi-parallel shocks waves, the reflected ions travel upstream along the magnetic field and escape from the bow shock. As they travel

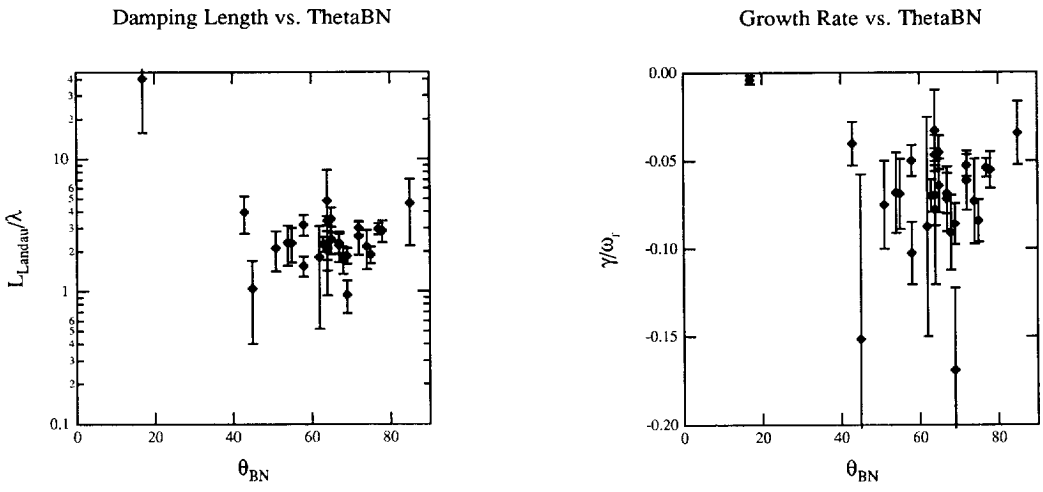

Fig. 12 Damping length measured in precursor wavelengths (left) and growth rate normalized by the real part of the frequency (right) as a function of the angle between the IMF and the shock normal.

upstream they flow counter to the incoming solar wind flow and generate a spectrum of waves which are discussed in detail elsewhere in this volume. Figure 13 shows an example of these waves seen right at the shock. We see that these upstream waves are convected through the shock and are amplified in this process. In fact the interaction of these upstream waves with the shock is very complex. Not only can they affect the particle reflection process that created the beams that generated the waves in the first place, but they can grow to shock-like amplitudes themselves. Moreover, even if they were to have small amplitudes the waves could undergo mode conversion upon convection through the shock [22].

We note that these processes which generate the upstream and downstream waves are all amplified as the Mach number increases. Figure 14 shows the broadband amplitude of downstream waves as the Mach number increases.

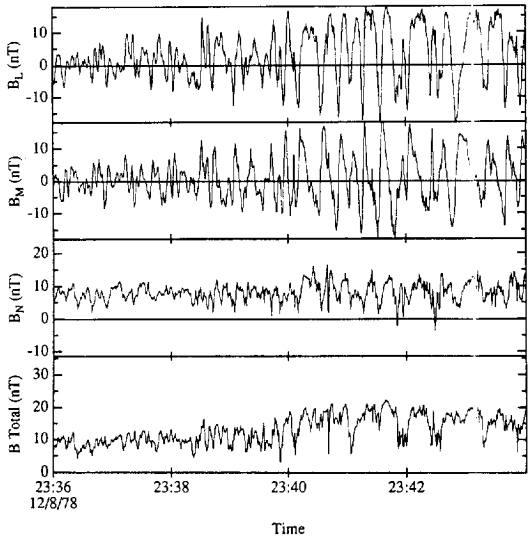

Fig. 13 Magnetic field measurements of a marginally critical, quasi-parallel shock in shock normal coordinates. Upstream conditions were M_{ms}=2.59, β=0.31 and θ_{BN} = 22°.

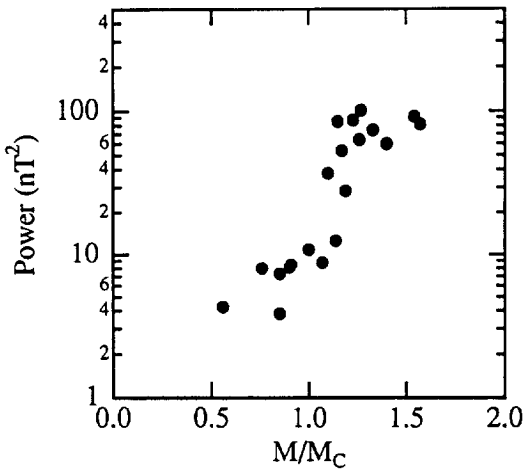

Fig. 14 Integrated downstream power versus ratio of criticality.

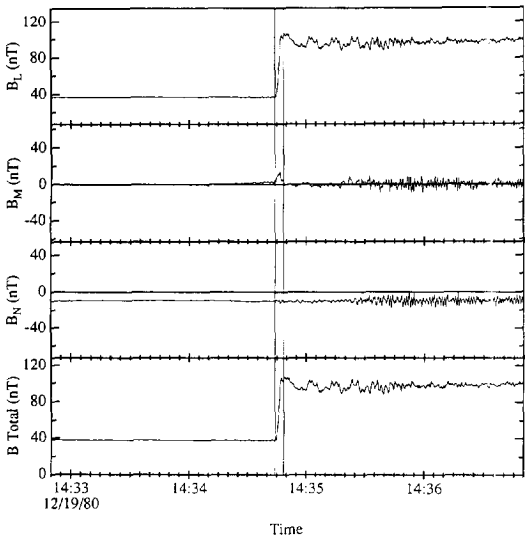

Fig. 15 Magnetic field measurements of a low beta, quasi-perpendicular marginally critical shock in shock normal coordinates. Upstream conditions were $M_{ms}=3.18$, $\beta=0.04$ and θ_{BN} = 75°.

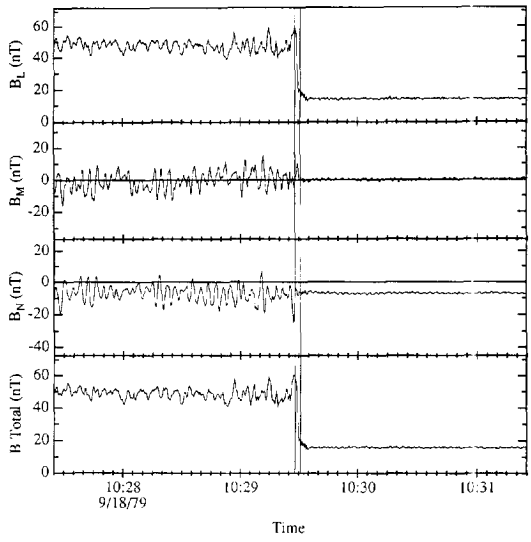

Fig. 16 Magnetic field measurements for a low beta, quasi-perpendicular supercritical shock in shock normal coordinates. Upstream conditions were M_{ms} = 2.71, $\beta=1.33$ and θ_{BN} = 62°.

DOWNSTREAM WAVES

In our above discussion we noted that at low Mach numbers waves could propagate upstream from the shock but as the Mach number increases these waves are swept downstream as are any waves generated away from the shock in the upstream region. However, there is yet another source of waves at the shock, those that grow downstream from the shock on the free energy supplied by the shocked particle distributions. Figure 15 shows an example of such waves for a marginally critical quasi perpendicular shock. Of particular interest are the high frequency waves along the M and N directions that are nearly perpendicular to the magnetic field that is mainly along the L direction. This transverse wave grows slowly with distance behind the shock. Also of note here is the periodic overshoot in the field magnitude which suggests that the reflected ions that drift back into the sheath remain coherent for some distance. Also of note is the non-coplanarity component in the M-component in the middle of the shock. Here the non-coplanarity is isolated from any upstream or downstream waves. This is in contrast to the subcritical shock shown in Figure 5 where the non-coplanarity component anchored the standing precursor in the shock.

At higher Mach numbers the waves are both stronger and more rapidly growing. Figure 16 shows a supercritical quasi perpendicular shock in boundary normal coordinates that illustrates this. Again the waves are largely transverse but do have a compressional component. We note that the non-coplanarity component is present with the expected polarity. It begins the train of downstream waves but its phase relation to these waves varies with time because the downstream waves are propagating away from the shock. We also see that there is a small foot in front of the shock ramp signifying the presence of reflected ions. If we increase beta to close to unity as illustrated in Figure 17, the wave behavior does not change substantially but the non-coplanarity component decreases as expected.

The statistical properties of these downstream waves are shown in Figures 18, 19 and 20. Generally the waves propagate at a small angle to the magnetic field, are nearly circularly polarized and propagate at close to the Alfven velocity. These properties identify them as ion cyclotron waves. We would expect such waves to arise because both adiabatic compression of the ion distributions across the shock and the ion reflection mechanism create distributions with greater perpendicular temperature than parallel temperature.

Inspection of Figures 18 and 19 show that some, but a minority, of the waves are probably not ion

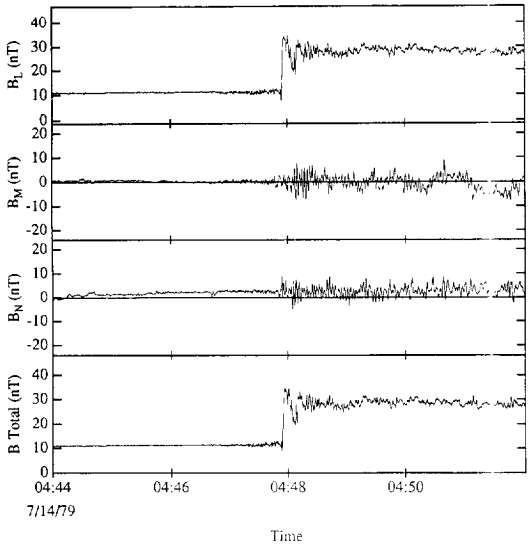

Fig. 17 Magnetic field measurements of a moderate beta, quasi-perpendicular shock with ion cyclotron waves in the downstream region on 7/14/79. Upstream conditions were $M_{ms}=3.81$, $\beta=1.15$ and $\theta_{BN}=76°$.

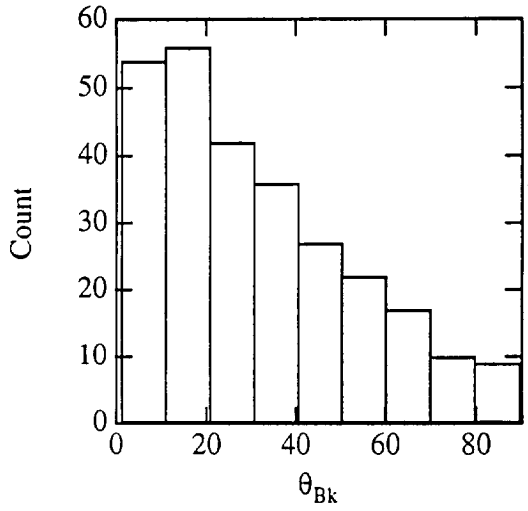

Fig. 18 Distributions of propagation angle for waves downstream of quasi perpendicular shocks.

cyclotron waves. These waves propagate at a large angle to the magnetic field and are linearly polarized. Figure 21 shows an example of a bow shock crossing for which such waves were present. As is evident from the bottom trace the waves are highly compressional. We identify these waves as mirror mode waves. In Figure 22 we show the conditions under which these waves and the ion cyclotron waves occur. The mirror mode waves occur when the helium content is high and the downstream beta is high. We interpret this result as due to the suppression of the ion cyclotron instability by the heavy ions as predicted by Price et al. [23]. This suppression appears only to be effective at high betas.

CONCLUSIONS

The Rankine Hugoniot relations which predict the downstream conditions from the upstream conditions

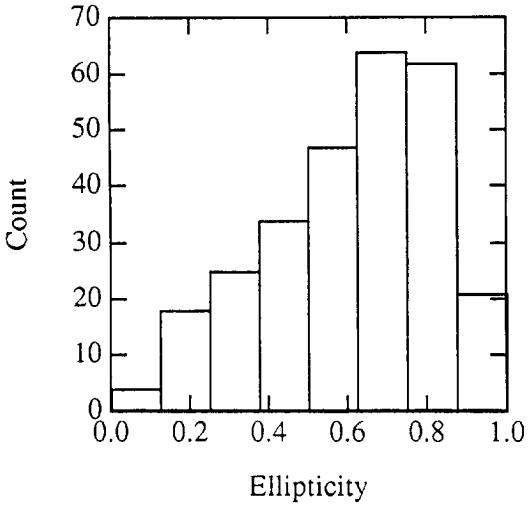

Fig. 19 Distributions of wave ellipticity for waves downstream of quasi-perpendicular shocks.

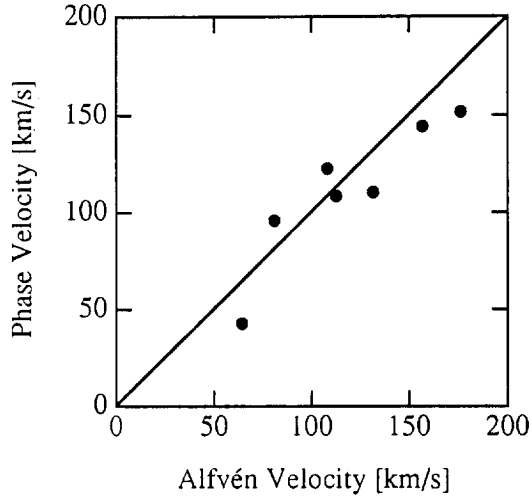

Fig. 20 Plasma rest frame phase velocity of downstream waves versus Alfven mode velocity.

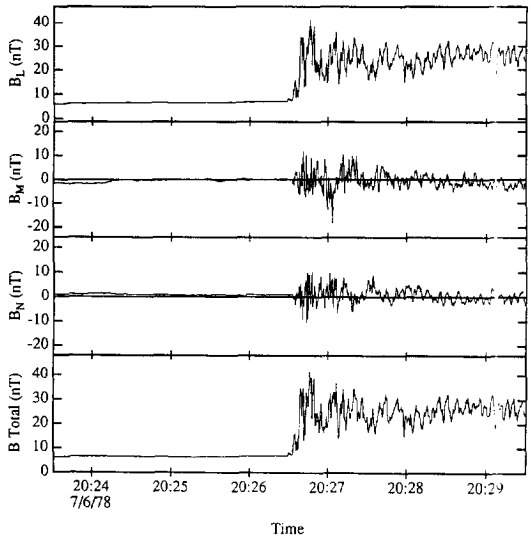

Fig. 21 Magnetic field measurements of a moderate beta quasi-perpendicular shock with mirror mode waves in the downstream region on 7/6/78. Upstream conditions were $M_{ms}=6.72$, $\beta=2.23$ and $\theta_{BN}=84°$.

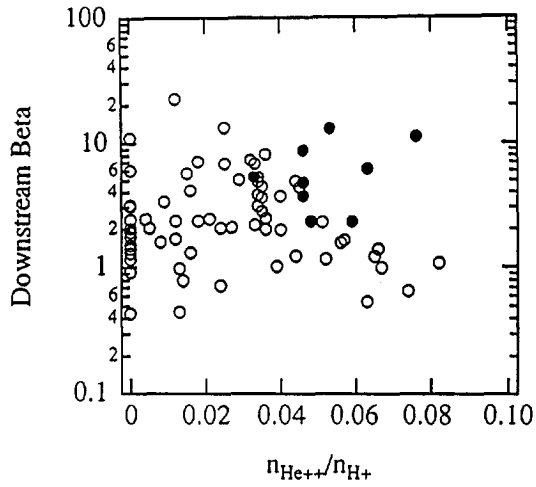

Fig. 22 Downstream beta versus solar wind helium content for quasi-perpendicular shocks used in wave analysis. Wave activity dominated by ion cyclotron waves is indicated by open circles. Wave activity dominated by mirror mode waves is indicated by closed circles.

depend on the Mach number of the flow the beta of the plasma and the angle between the upstream magnetic field and the shock normal. Although the Rankine-Hugoniot equations do not tell us about the micro processes that occur and that are required to provide the dissipation predicted by Rankine Hugoniot, it is these same three parameters that exert most of the control over these processes. The most important parameter is the Mach number of the shock. At low Mach numbers whistler mode waves can propagate upstream and two such whistler mode waves are seen. One is phase standing along the shock normal and Landau damps in the incoming solar wind. The other wave propagates more closely along the magnetic field and can propagate to much greater distances from the shock. We still do not understand clearly the source of this wave but speculate that it is associated with the electrons accelerated through the shock.

The Mach number also controls the ion reflection process and the strength of the ion anisotropies downstream from the shock. Thus as the Mach number increases ion cyclotron waves are found behind the shock. At highest Mach numbers, ion composition becomes important also and when the helium content exceeds about 4% by number, the ion cyclotron waves become suppressed and the mirror instability is allowed to grow.

The angle of the upstream magnetic field to the flow exerts control on the duration of the precursor at low Mach numbers. At higher Mach numbers this angle determines whether ions can travel upstream away from the shock. These ions, in turn, generate large amplitude waves as they counterstream in the solar wind. These waves are convected against the shock and most strongly affect the structure of the quasi parallel shock.

The plasma beta at first glance seems to have the least effect on the shock structure but it too seems to have important effects on the growth rates of the instabilities and may also be important for plasma waves at VLF frequencies which we have not covered in this review.

ACKNOWLEDGMENTS

This work was supported by the National Aeronautics and Space Administration under research grant NAGW-3477.

REFERENCES

1. D. A. Tidman and N. A. Krall, Shock Waves in Collisionless Plasmas, Interscience, New York, (1971).

2. M. H. Farris, C. T. Russell and M. F. Thomsen, Magnetic structure of the low beta quasi-perpendicular shock, *J. Geophys. Res. 98*, 15,285-15,294 (1993).

3. D. Winterhalter, M. G. Kivelson, R. J. Walker and C. T. Russell, Magnetic field change across the Earth's bow shock: Comparison between observations and theory, *J. Geophys. Res., 90*, 3925 (1985).

4. M. Tatrallyay, C. T. Russell, J. G. Luhmann, A. Barnes, and J. D. Mihalov, On the proper Mach number and ratio of specific heats for modeling the Venus bow shock, *J. Geophys. Res., 89*, 7381 (1984).

5. C. T. Russell, J. T. Gosling, R. D. Zwickl and E. J. Smith, Multiple spacecraft observations of interplanetary shocks: ISEE three dimensional plasma measurements, *J. Geophys. Res., 88*, 9941 (1983).

6. M. H. Farris, C. T. Russell, M. F. Thomsen and J. T. Gosling, ISEE 1 and 2 observations of the high betas shock, *J. Geophys. Res., 97*, 19121 (1992).

7. C. C. Goodrich and J. D. Scudder, The adiabatic energy change of plasma electrons and the frame dependence of the cross-shock potential at collisionless magnetosonic shock waves, *J. Geophys. Res., 89*, 6654 (1984).

8. F. C. Jones and D. C. Ellison, Noncoplanar magnetic fields, shock potentials and ion deflection, *J Geophys. Res., 92*, 11205 (1987).

9. M. F. Thomsen, J. T. Gosling, S. J. Bame, K. B. Quest, D. Winske, W. A. Livesey and C. T. Russell, On the noncoplanarity component of the magnetic field within a fast collisionless shock *J. Geophys. Res., 92*, 2305 (1987).

10.W. A. Livesey, The subcritical-to-supercritical transition in quasi-perpendicular fast shocks Ph.D. Thesis, University of California Los Angeles (1985).

11.M. A. Friedman, C. T. Russell, J. T. Gosling and M. F. Thomsen, Non-coplanar component of the magnetic field at low Mach number shocks, *J. Geophys. Res., 95*, 2441-2445 (1990).

12.M. H. Farris, C. T. Russell, R. J. Fitzenreiter and K. W. Ogilvie, The subcritical, quasi parallel (switch-on) shock, *Geophys. Res. Lett., 21*, 837-840 (1994).

13.C. T. Russell, D. D. Childers and P. J. Coleman, OGO-5 observations of upstream waves in the interplanetary medium, *J. Geophys. Res., 76*, 845-861 (1971).

14.D. H. Fairfield, Whistler waves observed upstream of collisionless shocks, *J. Geophys. Res., 79*, 1368-1378, 1974.

15.D. S. Orlowski, G. K. Crawford and C. T. Russell, Upstream waves at Mercury, Venus and Earth: Comparison of properties of one Hertz waves, *Geophys. Res. Lett. 17*, 2293-2296 (1990).

16.M. M. Hoppe, C. T. Russell, L. A. Frank, T. E. Eastman and E. W. Greenstadt, Upstream hydromagnetic waves and their association with backstreaming ion population: ISEE 1 and 2 observations, *J. Geophys. Res., 86*, 4471-4492, (1981).

17.D. D. Sentman, M. F. Thomsen, S. P. Gary, W. C. Feldman and M. M. Hoppe, The oblique whistler instability in the Earth's foreshock, *J. Geophys. Res., 89*, 2048-2056 (1983).

18.D. S. Orlowski, C. T. Russell, D. Krauss-Varban, and N. Omidi, On the source of upstream whistlers in the Venus foreshock, in Plasma Environments of Non-Magnetic Planets, edited by T. I. Gombosi, 217-227, Pergamon Press (1993).

19.D. S. Orlowski, C. T. Russell, D. Krauss-Varban, N. Omidi and M. F. Thomsen, On the source, formation and damping of broadband upstream whistlers, Adv. Space Res., this volume (1994).

20.D. S. Orlowski, C. T. Russell, and R. P. Lepping, Wave phenomena in the upstream region of Saturn, *J. Geophys. Res., 97*, 19187-19199 (1992).

21.S. P. Gary and M. M. Mellott, Whistler damping at oblique propagation: Laminar shock precursors *J. Geophys. Res. 90*, 99 (1985).

22.D. Krauss-Varban and N. Omidi, Propagation characteristics of waves upstream and downstream of quasi-parallel shocks, *Geophys. Res. Lett., 20*, 1007, (1993).

23.C. P. Price, D. W. Swift and L-C. Lee, Numerical simulation of non-oscillatory mirror waves at the Earth's magnetosheath, *J. Geophys. Res., 91*, 101, (1986).